

## Visualization of quantitative lipid distribution in mouse liver through near-infrared hyperspectral imaging: supplement

KYOHEI OKUBO,<sup>1,\*</sup>  YUICHI KITAGAWA,<sup>1</sup> NAOKI HOSOKAWA,<sup>1</sup>  
MASAKAZU UMEZAWA,<sup>1</sup>  MASAO KAMIMURA,<sup>1</sup>  TOMONORI  
KAMIYA,<sup>2</sup>  NAOKO OHTANI,<sup>2</sup>  AND KOHEI SOGA<sup>1</sup> 

<sup>1</sup>Department of Materials Science and Technology, Faculty of Industrial Science and Technology, Tokyo University of Science, 6-3-1 Niijuku, Katsushika-ku, Tokyo 125-8585, Japan

<sup>2</sup>Department of Pathophysiology, Graduate School of Medicine, Osaka City University, 1-4-3 Asahi-machi, Abeno-ku, Osaka 545-8585, Japan

\*kyohei.okubo@rs.tus.ac.jp

---

This supplement published with The Optical Society on 12 January 2021 by The Authors under the terms of the [Creative Commons Attribution 4.0 License](#) in the format provided by the authors and unedited. Further distribution of this work must maintain attribution to the author(s) and the published article's title, journal citation, and DOI.

Supplement DOI: <https://doi.org/10.6084/m9.figshare.13557275>

Parent Article DOI: <https://doi.org/10.1364/BOE.413712>

# Visualization of quantitative lipid distribution in mouse liver through near-infrared hyperspectral imaging: supplemental document

**Table S1.** Detailed information on the mouse liver samples used for regression modelling (serial nos.: 1–75), including the strain, age (in weeks), food, liver weight, as well as the lipid contents measured using the Folch extraction method and estimated using the SVR model.

Group	Serial no.	Strain	Age (week)	Food	Liver weight (g)	Lipid content (mg/g)	
						Folch extraction	SVR estimation
A	1	C57BL/6NJcl	31	CE-2	0.101	32.61	46.98
A	2	C57BL/6NJcl	31	CE-2	0.191	35.70	47.16
A	3	C57BL/6NJcl	31	CE-2	0.107	40.26	40.04
A	4	ICR	35	CE-2	0.136	46.49	79.37
A	5	ICR	28	CE-2	0.619	46.51	56.94
A	6	ICR	35	CE-2	0.270	46.67	61.69
A	7	ICR	28	CE-2	0.373	48.82	54.36
A	8	C57BL/6NJcl	31	CE-2	0.137	53.13	60.67
A	9	ICR	35	CE-2	0.523	53.20	56.83
A	10	ICR	28	CE-2	0.689	53.85	53.30
A	11	C57BL/6NJcl	31	CE-2	0.112	57.30	57.74
A	12	ICR	35	D12492, 4w	0.397	64.82	81.86
A	13	C57BL/6NJcl	31	D17011207, 30w	0.193	66.18	67.56
A	14	ICR	35	D12492, 4w	0.183	66.56	85.28
A	15	ICR	35	D12492, 4w	0.629	67.59	73.89
B	16	ICR	35	CE-2	0.280	71.33	78.44
B	17	ICR	35	CE-2	0.345	72.17	84.39
B	18	ICR	8	D12492, 4w	0.435	79.31	93.16
B	19	ICR	8	D12492, 4w	0.408	79.72	93.28
B	20	ICR	35	CE-2	0.153	83.01	91.93
B	21	C57BL/6NJcl	31	D17011207, 30w	0.165	93.28	92.10
B	22	ICR	8	D12492, 4w	0.457	95.58	94.12
B	23	ICR	8	D12492, 4w	0.450	96.31	97.77
B	24	C57BL/6NJcl	31	D17011207, 30w	0.151	96.75	95.02
B	25	ICR	6	D12492, 2w	0.370	98.08	92.37
B	26	ICR	6	D12492, 2w	0.478	101.88	96.94
B	27	ICR	6	D12492, 2w	0.418	102.13	98.09
B	28	C57BL/6NJcl	31	D17011207, 30w	0.185	102.76	96.93
B	29	ICR	35	D12492, 4w	0.459	112.71	116.99
B	30	ICR	35	D12492, 4w	0.118	114.96	137.48

C	31	ICR	5	D12492, 1w	0.675	139.56	146.00
C	32	ICR	35	D12492, 4w	0.115	143.23	163.41
C	33	C57BL/6NJcl	31	D17011207, 30w	0.281	157.76	136.72
C	34	ICR	5	D12492, 1w	0.558	159.03	160.30
C	35	ICR	5	D12492, 1w	0.699	160.85	167.10
C	36	ICR	5	D12492, 1w	0.962	170.13	161.40
C	37	C57BL/6NJcl	31	D17011206, 30w	0.173	179.77	175.99
C	38	C57BL/6NJcl	31	D17011206, 30w	0.362	179.96	206.40
C	39	ICR	8	D12492, 4w	0.479	195.08	185.97
C	40	C57BL/6NJcl	31	D17011206, 30w	0.181	195.24	192.35
C	41	ICR	6	D12492, 2w	0.791	197.42	216.90
C	42	ICR	28	CE-2	0.717	201.51	245.57
C	43	ICR	28	CE-2	1.098	204.30	251.36
C	44	C57BL/6NJcl	35	D12492, 34w	0.303	204.42	224.40
C	45	ICR	8	D12492, 4w	0.590	207.39	192.32
D	46	ICR	8	D12492, 4w	0.433	207.86	199.03
D	47	ICR	8	D12492, 4w	0.522	214.33	218.78
D	48	C57BL/6NJcl	35	D12492, 34w	0.554	216.10	248.94
D	49	C57BL/6NJcl	35	D12492, 34w	0.802	218.69	199.34
D	50	C57BL/6NJcl	21	D12492, 21w	0.280	223.45	231.17
D	51	ICR	6	D12492, 2w	0.629	231.19	211.40
D	52	C57BL/6NJcl	21	D12492, 21w	0.154	232.12	233.27
D	53	C57BL/6NJcl	21	D12492, 21w	0.460	234.50	246.93
D	54	ICR	6	D12492, 2w	0.647	243.66	239.70
D	55	C57BL/6NJcl	21	D12492, 21w	0.270	244.26	248.55
D	56	C57BL/6NJcl	21	D12492, 21w	0.281	244.75	246.67
D	57	C57BL/6NJcl	31	D17011206, 30w	0.196	245.52	247.88
D	58	ICR	28	CE-2	0.710	246.69	246.48
D	59	ICR	28	CE-2	0.754	250.80	230.56
D	60	ICR	28	CE-2	0.905	250.88	245.80
E	61	C57BL/6NJcl	35	D12492, 34w	0.366	251.03	268.88
E	62	ICR	6	D12492, 2w	1.134	255.69	221.10
E	63	C57BL/6NJcl	21	D12492, 21w	0.443	256.94	251.07
E	64	C57BL/6NJcl	35	D12492, 34w	0.858	261.27	240.01
E	65	C57BL/6NJcl	31	D17011206, 30w	0.243	261.86	257.74
E	66	C57BL/6NJcl	21	D12492, 21w	0.306	268.60	272.28
E	67	C57BL/6NJcl	21	D12492, 21w	0.177	268.88	267.14
E	68	C57BL/6NJcl	21	D12492, 21w	0.260	269.59	263.49
E	69	C57BL/6NJcl	21	D12492, 21w	0.450	270.87	264.38
E	70	C57BL/6NJcl	21	D12492, 21w	0.451	277.36	260.67
E	71	C57BL/6NJcl	21	D12492, 21w	0.106	287.46	268.67
E	72	C57BL/6NJcl	21	D12492, 21w	0.154	289.80	273.70

E	73	C57BL/6NJcl	21	D12492, 21w	0.387	293.46	277.17
E	74	C57BL/6NJcl	21	D12492, 21w	0.330	295.21	289.36
E	75	C57BL/6NJcl	21	D12492, 21w	0.411	296.76	290.10

---

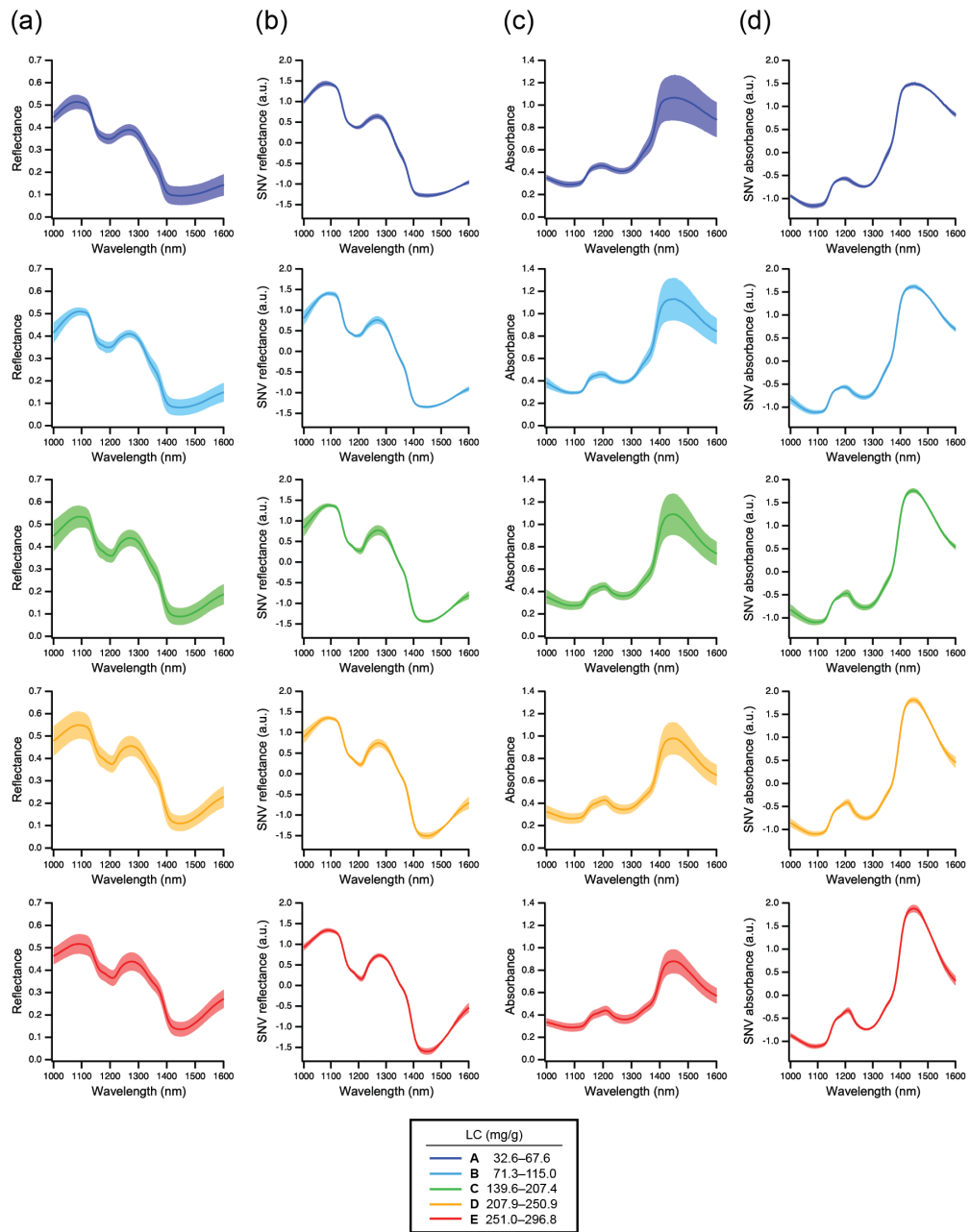


**Fig. S1.** Averaged spectra of the (a) reflectance, (b) reflectance with SNV, (c) absorbance, and (d) absorbance with SNV. The solid lines and shaded areas indicate the mean value and standard deviation of the profiles, respectively.

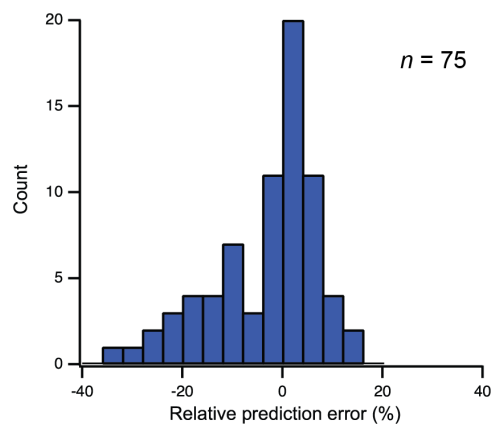


**Fig. S2.** Histogram of the relative prediction errors (%).